Speciation of Cu cations in Cu-CHA catalysts for NH$_3$-SCR:

the effects of SiO$_2$/AlO$_3$ ratio and Cu-loading

investigated by transient response methods

R. Villamaina[1], Shaojun Liu[1], I. Nova[1], E. Tronconi[1],*

M. P. Ruggeri[2], J. Collier[2], A. York[2], D. Thompsett[2]

[1]*Laboratory of Catalysis and Catalytic Processes, Dipartimento di Energia, Politecnico di Milano,*

via La Masa 34, 20156 Milan, Italy

[2]*Johnson Matthey Technology Centre, Blounts Court Road, Sonning Common, Reading RG4 9NH,*

UK

*enrico.tronconi@polimi.it

Abstract: We develop an experimental protocol to quantify the speciation of Cu ions (ZCu^{II}OH and Z$_2$Cu^{II}) in Cu-CHA catalysts for the NH$_3$ Selective Catalytic Reduction of NOx (NH$_3$-SCR). To this purpose, we performed four transient tests, namely H$_2$-TPR, NO+NH$_3$ TPR, NO$_2$ adsorption + TPD and NH$_3$ adsorption +TPD, over two sets of Cu-CHA research catalysts characterized by different Cu contents (0-2.1% w/w) and SiO$_2$/Al$_2$O$_3$ (SAR) ratios (10-25).

Preliminary H$_2$-TPR tests on the samples with the extreme SAR and Cu loading values were used to identify the variability range of the fractions of ZCu^{II}OH and Z$_2$Cu^{II} species in these catalysts. The ZCu^{II}OH fraction was found to vary between 0.55 (at Cu/Al = 0.11) and 0.79 (at Cu/Al = 0.29).

NO+NH$_3$ TPR runs demonstrated that the NO+NH$_3$ mixture is a much stronger reducing agent than H$_2$: full reduction of all the Cu was obtained already at lower temperature, and differences in the reducibility of ZCu^{II}OH and Z$_2$Cu^{II} were strongly attenuated. Both the integral NO consumption and

1

the integral N_2 release were found to be effective estimators of the reducible Cu in Cu-CHA, matching the total Cu from ICP measurements.

NO_2 adsorption + TPD tests pointed out that NO_2 is adsorbed in the form of nitrates on $ZCu^{II}OH$ ions only, the nitrates storage capacity being therefore dependent on SAR and Cu loading: on increasing both parameters, the amount of stored NO_x increased, as well as their stability. Both the NO released during isothermal NO_2 adsorption and the NO_2 released during the following TPD can be used to directly estimate the number of $ZCu^{II}OH$ ions in Cu-CHA.

Finally, NH_3-TPD provided information on the acid sites in the Cu-CHA samples. From the NH_3 stored on Lewis sites, it was possible to evaluate the number of NH_3 molecules coordinated to each Cu atom: a decrease of the NH_3/Cu ratio on increasing both SAR and Cu content was observed. This behaviour is explained by the changes in the distribution of $ZCu^{II}OH$ and Z_2Cu^{II} sites in Cu-CHA, as a result of varying the Cu/Al ratio. In accordance with literature results, we found that Cu ions are able to ligate either 3 ($ZCu^{II}OH$) or 4 (Z_2Cu^{II}) NH_3 molecules, when gaseous NH_3 is present, the NH_3/Cu ratios estimated from our experiments falling close to this range. When only preadsorbed NH_3 was present, however, (no gaseous ammonia), the NH_3/Cu ratio dropped to either 1 ($ZCu^{II}OH$) or 2 (Z_2Cu^{II}). Based on these elements, NH_3 TPD can also be used to quantify the two Cu species in Cu-CHA. We recommend however the more straightforward approach based on i) NO + NH_3 TPR (for direct quantification of the overall reducible Cu) and ii) NO_2 TPD (for direct quantification of the $ZCu^{II}OH$ species).

1. Introduction

The Selective Catalytic Reduction (SCR) with NH_3/urea is nowadays considered the most effective technology for the abatement of NO_x emissions from Diesel and other lean burn engines [1]. Among the catalysts available for this technology, Cu exchanged zeolites have proven to be excellent catalysts due to their very high $DeNO_x$ activity, especially at low temperatures, a fundamental prerequisite to meet the current NO_x emission limitations, and to their superior hydrothermal stability and low selectivity to N_2O [2–7]. The porous structure of the Cu-promoted zeolite catalysts was demonstrated to have a fundamental role in the activity towards SCR reactions [6]. Among the available zeolite materials the Cu-CHA structure was recognized as the best lean NO_x abatement catalyst on the market, showing improved low temperature NO conversion and N_2 selectivity in comparison with those with larger pores [8–10]. Cu-CHA catalysts have been widely investigated by several research groups and it is generally agreed that isolated Cu ions located at the exchange sites are the main contributors to the SCR reactions [11–14]. However, a few aspects remain still debated, such as the nature of the Cu catalytic centers, their activity towards SCR reactions and their dependence on catalyst formulation parameters (Si/Al and Cu/Al ratios). The existence of two distinct Cu ions populations within the CHA framework has been probed in the literature by means of different techniques, such as X-ray diffraction (XRD) [15,16], X-ray absorption and emission spectroscopy (XAS and XES) [11,17], FTIR/DRIFTS [16,17] and electron paramagnetic resonance (EPR) [7]. Specifically, Paolucci et al. [11] showed that the exchanged Cu^{II} ions within the CHA cages can populate two distinct types of sites, differentiated by the number of charge-compensating Al atoms: Z_2Cu^{II}, where Cu^{II} ions are doubly coordinated with the Al atoms of the zeolite framework, and $ZCu^{II}OH$, in which Cu^{II} ions are singly coordinated with the zeolite framework. Combined computational and experimental analysis of zeolites over a wide range of chemical compositions demonstrated the speciation of Cu sites to be related to the Si/Al and Cu/Al ratios [11]. Gao et al. [12] observed the existence of multiple Cu^{II} sites characterized by different locations and redox properties, which can be systematically tuned by adjusting Si/Al and Cu/Al values of Cu promoted SSZ-13 catalysts, as confirmed recently by Fan et

al. [7] through EPR and H_2-TPR runs. Besides, evidence of the presence of two different Cu species was given also by Luo et al. [9]: they observed a transformation of Cu sites from $ZCu^{II}OH$ to Z_2Cu^{II} on Cu-CHA catalysts subjected to progressive hydrothermal aging through DRIFT, NH_3-TPD and H_2-TPR experiments.

In this work we investigate the effect of SiO_2/Al_2O_3 ratio and Cu loading on some fundamental properties of Cu-CHA catalysts for the NH_3-SCR process, such as the interaction of NH_3 and nitrates adspecies with the Cu ions and their reducibility, all of them possibly affecting the SCR activity. Four types of transient tests were designed to investigate the aforementioned catalytic properties, namely H_2-TPR, $NO+NH_3$ TPR, NO_2 adsorption + TPD and NH_3 adsorption + TPD. The results provide converging evidence of the existence of the two Cu cations within the Cu-CHA catalysts and of their dependence on SAR and Cu loading. Furthermore, herein we demonstrate that a combination of simple and well-established transient response methods enables an effective quantitative characterization of the Cu species in Cu-CHA under realistic conditions for the NH_3-SCR reactions, in contrast to the more sophisticated spectroscopic techniques already proposed in literature.

2. Experimental

2.1 Catalyst samples and experimental setup

Two sets of Cu-exchanged chabazite (Cu-CHA) model catalysts, directly provided in the form of powders by Johnson Matthey, were tested. One set contains five samples with different SiO_2/Al_2O_3 (SAR) ratios over the range 10-25 but with the same Cu loading (1.7% w/w); the second one consists of four samples with same SAR (25) but with different Cu loadings (0-2.1% w/w). Table 1 reports the actual Cu loading (w/w) measured by ICP-MS analysis of each sample. The Cu/Al ratios are based on the measured Cu loading. UV-Vis spectra confirmed the absence of un-exchanged Cu or CuOx species in all the tested catalyst samples.

Table 1. List of powder catalysts

Sample	%Cu (w/w) ICP-MS analysis	SAR	Cu/Al
1.7Cu-CHA10	1.7	10	0.12
1.7Cu-CHA13	1.7	13	0.17
1.7Cu-CHA17	1.7	17	0.21
1.7Cu-CHA22	1.7	22	0.22
CHA25	/	25	0
0.7Cu-CHA25	0.7		0.11
1.7Cu-CHA25	1.7		0.24
2.1Cu-CHA25	2.1		0.29

The samples were conditioned with heating them up to 600 °C at 5 °C/min and holding the maximum temperature for 5 hours, while feeding 10% O_2 and 10% H_2O.

16 mg of catalyst powder, diluted up to 130 mg with cordierite, were loaded in a quartz reactor (6 mm ID) and suspended by means of quartz wool. To enhance the gas mixing, beds of quartz grains were placed upstream and downstream of the catalyst powder. The reactor was inserted in a vertical electric furnace and its temperature was controlled by a K-type thermocouple directly immersed in the catalyst bed.

Helium was used as balance gas in all the micro-reactor runs. Gases were dosed using mass flow controllers (Brooks Instruments). Temporal evolution of the species at the reactor outlet was followed using a mass spectrometer (QGA Hiden Analytical) and a UV analyzer (ABB LIMAS 11 HW) in a parallel configuration, which allowed the simultaneous measurement of NO, NO_2, NH_3, N_2 and N_2O.

2.2 Catalyst characterization tests

H_2-TPR experiments were performed on three specific samples, 1.7Cu-CHA10 (lowest SAR), 0.7Cu-CHA25 (lowest Cu loading), 2.1Cu-CHA25 (highest SAR and highest Cu loading), in order to obtain direct estimates of the fractions of $ZCu^{II}OH$ and Z_2Cu^{II} sites. The two species, indeed, showed very distinct reduction temperatures in H_2 [9,18]. The samples (about 100 mg) were first pre-oxidized in a stream of 2.05% O_2 in He (20 Ncc/min) at 550°C for 1 hour. Then the samples ware

5

cooled down to room temperature and after a purge of 15 minutes the TPR run started. During the TPR the feed stream included 5% v/v H_2 in Ar (20 Ncc/min) and the temperature was increased up to 600°C with a heating rate of 10 °C/min.

Temperature-programmed reduction (TPR) was also performed using a mixture of NH_3 and NO as an alternative reductant to H_2. The TPR experiment was carried out by ramping the temperature from 80 to 550 °C at a heating rate of 10 °C/min while feeding a gaseous stream containing 500 ppm of NO and 500 ppm of NH_3 in He, with a GHSV equal to 266250 $cm^3/(g_{cat}*h)$ STP. During the experiment both the consumption of NO and the production of N_2 were monitored to estimate the reducibility of Cu ions under operating conditions closer to the SCR process.

The interaction between NH_3 molecules and the catalyst centers, the amount of acid sites and their distribution were studied by NH_3 adsorption + temperature programmed desorption (TPD) runs. The experiment is composed of three stages: (i) an isothermal NH_3 adsorption phase at 150 °C in which 500 ppm of NH_3 in He (GHSV= 266250 $cm^3/(g_{cat}*h)$ STP) was fed to the reactor, (ii) an isothermal desorption phase when the NH_3 feed was switched off after catalyst saturation, and (iii) an NH_3 desorption phase (TPD) in which the temperature was linearly increased up to 550 °C with a heating rate of 15 °C/min in He feed.

The same procedure was used to study the interaction of NO_x species with the catalyst surface. Thus, NO_2 adsorption + TPD tests were carried out, saturating the catalyst with 500 ppm NO_2/He at 120 °C (GHSV= 450000 $cm^3/(g_{cat}*h)$ STP) and, after the isothermal physi-desorption phase of 1 hour, the catalysts were heated from 120 to 550 °C at a rate of 15°C/min.

Prior to all the tests, the samples were pre-treated at 550°C feeding 8% O_2 in He for 1 hour, then cooled down to the starting temperature of the specific test under the same gas feed and finally purged with He for 15 min in order to control the oxidation state of the catalysts.

3. Results and discussion

3.1 H_2 – TPR

SAR and Cu/Al ratio are two catalyst parameters which affect the population of Cu ions in the zeolite framework. A known method used to estimate the fractions of Z_2Cu^{II} and $ZCu^{II}OH$ in Cu-CHA is H_2-TPR [9,12,13,18–20]. Indeed, these two Cu ions are characterized by a different reducibility, which therefore enables their unequivocal qualitative and quantitative determination. In this work H_2-TPR experiments were carried out on three samples associated with the extreme values of SAR and Cu loading for the Cu-CHA samples herein investigated. Accordingly, we herein evaluate the range over which the distribution of the two Cu ions varies in our catalysts when changing either SAR or Cu loading.

Figure 1 shows the H_2-TPR results, expressed in terms of rates of H_2 consumption [mmol/(s*g_{cat})] against temperature, on the 1.7Cu-CHA10 (lowest SAR, intermediate Cu loading), 0.7Cu-CHA25 (highest SAR, lowest Cu loading) and 2.1Cu-CHA25 (highest SAR and Cu loading) samples. All the samples exhibit a well-defined low-T peak, centred around 205-220°C, whose intensity depends on the Cu content (lowest on 0.7Cu-CHA25 and highest on 2.1Cu-CHA25). A peak centred at this low temperature is ascribed to the reduction of the $ZCu^{II}OH$ species [9,12,13,18,20]. Therefore, the first main consideration is that all the tested catalysts are characterized by the presence of $ZCu^{II}OH$ species independently of the SAR and of the Cu loading. On the other hand, another feature is visible at higher temperature (300-350 °C). For the 1.7Cu-CHA10 and 0.7Cu-CHA25 samples a well distinct peak is apparent, while for the 2.1Cu-CHA25 only a small shoulder is noted. This feature is instead assigned to Z_2Cu^{II} [9,12,13,18,20]. Such a Cu species, doubly coordinated with two Al sites of the CHA framework, is in fact more stable than $ZCu^{II}OH$, which is singly coordinated to one Al site, and is therefore associated with a higher reduction temperature [9,11,18,20]. When CHA zeolites are exchanged with Cu ions, the cages with two Al sites are firstly saturated by Cu, being the Z_2Cu^{II} species thermodynamically more stable than $ZCu^{II}OH$ [11]. Therefore (i) the lower the SAR, the higher the Al content resulting potentially

in a higher fraction of cages with two Al sites that can be saturated by Cu atoms as Z_2Cu^{II}; (ii) the lower the Cu loading the more important becomes the fraction of Z_2Cu^{II} with respect to the total number of Cu sites, whatever the Al content of the zeolite.
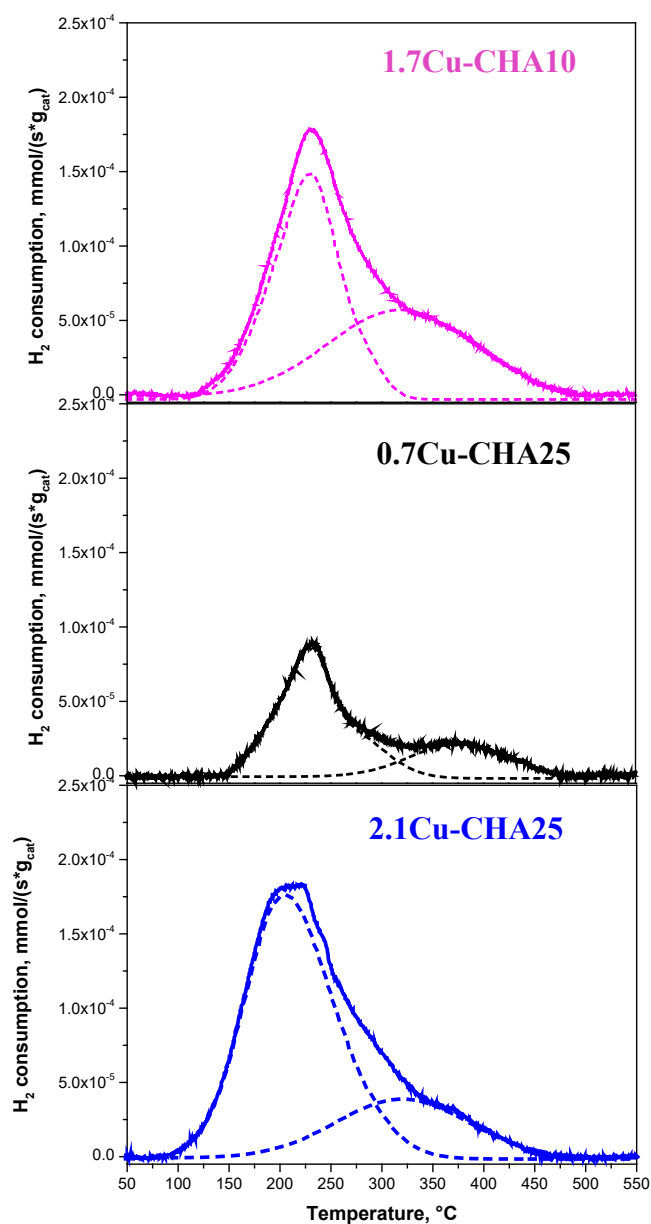

Figure 1. H_2-TPR on 1.7Cu-CHA10, 0.7Cu-CHA25 and 2.1Cu-CHA25 samples. Q=20 Ncc/min, H_2=5%, Ar. Heating rate= 10 °C/min. Pre-oxidized catalysts.

The bimodal profile of the H_2-TPR curves were fitted with a Gaussian function (experimental error within +/-5%) in order to estimate the fraction of both types of Cu sites. Table 2 shows the good

match between the sum of the deconvoluted signals and the experimental H_2 consumption. According to the following reduction stoichiometry

$$ZCu^{II}OH + \tfrac{1}{2}\,H_2 \rightarrow ZCu^{I} + H_2O \qquad\qquad (1)$$

$$Z_2Cu^{II} + \tfrac{1}{2}\,H_2 \rightarrow ZCu^{I} + ZH^{+} \qquad\qquad (2)$$

it is possible to quantify the amount of Cu ions reduced during the H_2-TPR experiment: these values match very well with the total amount of Cu present in each catalyst sample (estimated through ICP analysis). Consequently, all the Cu ions are reduced to Cu^{I}.

Table 2. Comparison between the experimental H_2 consumption and the sum of the deconvoluted signals and comparison between reduced Cu ions by H_2-TPR and total amount of Cu ions (by ICP) in 1.7Cu-CHA10, 0.7Cu-CHA25 and 2.1Cu-CHA25 samples

Sample	Peak1+Peak2 [µmol]	H_2 consumption [µmol]	Cu tot [µmol] (2*H_2 cons.)	Cu tot [µmol] (ICP)
1.7Cu-CHA10	13.1	13.6	27.2	27.0
0.7Cu-CHA25	5.7	5.6	11.3	11.1
2.1Cu-CHA25	14.5	14.6	29.2	29.5

Table 3, instead, reports the fractions of the two Cu species in the three samples, estimated by the same H_2-TPR fit. All the samples are characterized by the presence of $ZCu^{II}OH$ sites. The catalysts with low SAR and low Cu loading show similar fractions of the two Cu species, as expected from the theoretical predictions of Paolucci et al. [11]. However, according to [11] the expected number of $ZCu^{II}OH$ sites for Cu-CHA samples with those Si/Al and Cu/Al ratios would be lower than found from our H_2-TPR data. The differences from theory[11] may be ascribed to the practical difficulty to achieve an ideal Al distribution during the CHA synthesis. Therefore, even if in presence of high Al contents, the CHA framework may still contain cages with only one Al and in turn with a high fraction of ZCuOH sites.

Table 3. Populations of Z_2Cu^{II} and $ZCu^{II}OH$ in 1.7Cu-CHA10, 0.7Cu-CHA25 and 2.1Cu-CHA25 samples

Sample	SAR	Cu/Al	Z_2Cu^{II}	$ZCu^{II}OH$
1.7Cu-CHA10	10	0.12	44%	56%
0.7Cu-CHA25	25	0.11	45%	55%
2.1Cu-CHA25	25	0.29	21%	79%

The other catalyst samples tested for this work are characterized by SAR in the 10-25 range and with an intermediate Cu loading of 1.7 %. Consequently, the fractions of the two Cu ions are expected to vary between 21-45% for Z_2Cu^{II} and 55-79% for the $ZCu^{II}OH$ species.

3.2 NO+NH₃ TPR

From the H_2-TPR test we observed that Cu-CHA catalysts exhibit different reducibility properties which depend on the proportions of the two Cu species. By this experiment, two different reduction temperatures were identified, namely a lower one for the samples prepared with high SAR or high Cu loading (in which the population of $ZCu^{II}OH$ is maximized) and a higher one for samples with low SAR or low Cu content (characterized by the prevalence of Z_2Cu^{II} sites). Thus, ions singly coordinated with the framework are more easily reduced than those doubly bound to the CHA framework. However, the reducibility of the Cu ions is also affected by the nature of the reducing agent. Since NO and NH_3 are the reactants of the NH_3-SCR reactions, and knowing that their mixture has strong reducing properties, the TPR tests were repeated using this mixture in alternative to H_2 in order to study the reducibility properties of Cu ions under conditions closer to those of the SCR process. In fact, under SCR conditions at low temperatures the Cu ions are expected to be coordinated with NH_3 and/or H_2O, while during H_2-TPR test Cu species are only bond to the zeolite, and therefore they are not representative of the Cu ions properties under real SCR conditions [21].

After the usual pre-oxidation treatment, a stream of 500 ppm of NO and 500 ppm of NH_3 was fed to the reactor at 80 °C and then the temperature was ramped up to 550 °C at a heating rate of 10 °C/min. Only the initial part of the ramp (80-300 °C) is shown in Figure 2 (SAR effect) and Figure 3 (Cu loading effect), since above 300 °C the Slow SCR reaction (3) [22] lights off in the absence of oxygen,

$$6NO + 4NH_3 \rightarrow 5N_2 + 6H_2O \tag{3}$$

which is not relevant for the present study.

The data from the NO + NH$_3$ reduction runs are plotted in Figure 2 and 3 as NO consumptions and N$_2$ productions against temperature. The negative (NO) and positive (N$_2$) peaks observed in the Figures are the result of the reduction of the initially oxidized Cu ions, which occurs here already at very low temperatures. The comparison of the peak temperatures observed over samples with different SAR (Figure 2) and different Cu loadings (Figure 3) gives information about the reducibility of the catalyst samples characterized by different fractions of the two Cu sites. In particular, based on Paolucci et al. [11] and on our own results given in the previous section, we know that the increase of either SAR or Cu loading leads to an increased fraction of ZCu^{II}OH, which are more reducible species [9,21]. Concerning the SAR effect, shown in Figure 2, a slight difference in the peak temperature (about 20 °C) between the samples with lower SAR (10, 13) and higher SAR (17, 22, 25) was in fact observed. This result is in line with the H$_2$-TPR experiments: samples with a lower fraction of ZCu^{II}OH (low SAR) show a higher reduction temperature, indicating that Cu ions doubly coordinated with the CHA framework are more difficult to reduce. Under these operating conditions the reduction temperatures obtained by varying SAR are however very similar and closer compared to those found when using H$_2$ as a reducing agent, probably due to the presence of solvating NH$_3$ which lessens the differences between the reaction pathways and the activation barriers for the reduction of both Cu sites [11].
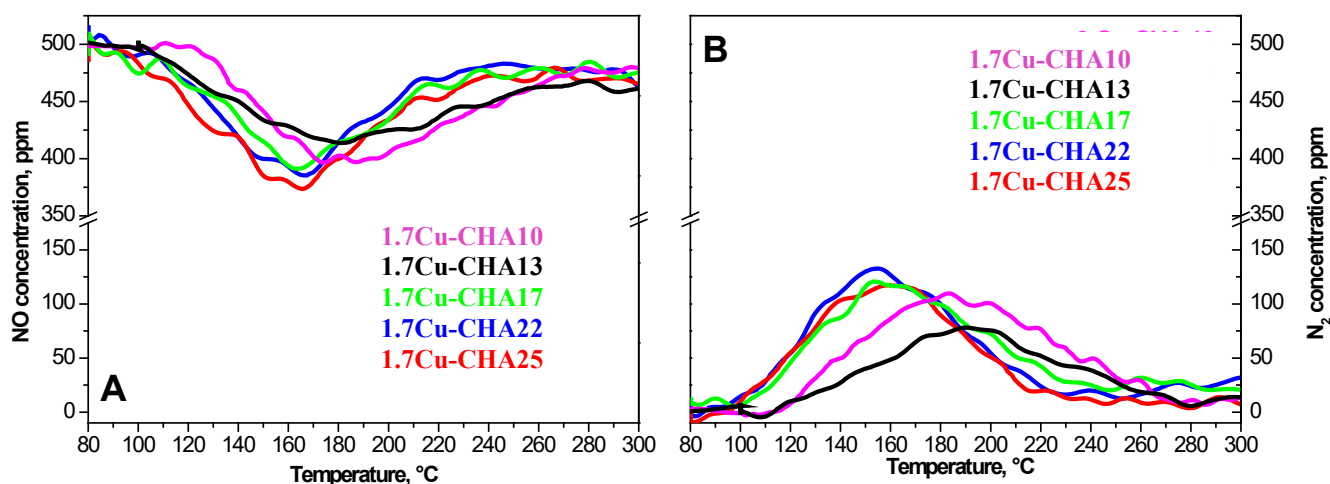
Figure 2. NO+NH$_3$ TPR runs performed over Cu-CHA catalysts with Cu loading= 1.7% w/w and different SARs (10, 13, 17, 22, 25): A) NO consumption, B) N$_2$ production. NH$_3$= 500 ppm, NO= 500 ppm, H$_2$O= 0% v/v, O$_2$= 0% v/v, heating rate= 10 °C/min, GHSV= 266250 cm^3/(g$_{cat}$*h) STP. Pre-oxidized catalysts.

The same behavior was expected for the Cu-CHA samples with different Cu contents: in fact, the [ZCu^{II}OH]/[Z$_2$Cu^{II}] ratio grows on increasing the Cu loading, therefore the samples with higher Cu content should be associated with reduction peaks centered at lower temperatures. Figure 3 shows exactly what is expected: the 1.7Cu-CHA25 and 2.1Cu-CHA25 samples exhibit peaks of NO consumption and N$_2$ formation centered around 160°C, while 0.7Cu-CHA25 is characterized by weaker peak at around 190 °C. Obviously, the intensities of the NO and N$_2$ peaks obtained over the 0.7Cu-CHA25 sample are considerably smaller than those of 1.7 and 2.1Cu-CHA 25 samples due to the smaller number of exchanged Cu sites.
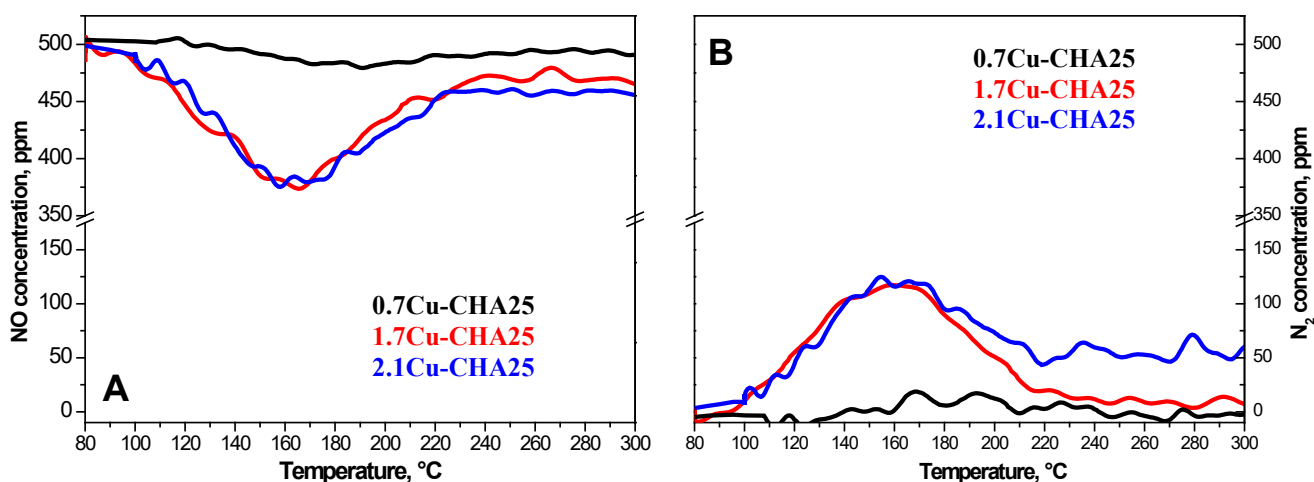
Figure 3. Comparison of NO+NH$_3$ TPR runs performed over Cu-CHA catalysts with SAR=25 and different Cu loadings (1-3 % w/w). A) NO consumption, B) N$_2$ production. NH$_3$= 500 ppm, NO= 500 ppm, H$_2$O= 0% v/v, O$_2$= 0% v/v, heating rate= 10 °C/min, GHSV= 266250 cm^3/(g$_{cat}$*h) STP. Pre-oxidized catalysts.

The reduction of Cu sites with the NO+NH$_3$ mixture occurs according to the following stoichiometries:

$$ZCu^{II}OH + NO + NH_3 \rightarrow ZCu^I + N_2 + 2H_2O \qquad (4)$$

$$Z_2Cu^{II} + NO + NH_3 \rightarrow ZCu^I + ZH + N_2 + H_2O \qquad (5)$$

Remarkably, whichever type of Cu site is present in Cu-CHA, for each reduced Cu ion one NO and one NH$_3$ molecules are consumed, with the corresponding formation of one N$_2$ molecule. Therefore, through the temporal integration of the dynamics of the NO consumption, or of the N$_2$ production, it is possible to estimate the amount of Cu ions reduced during the TPR experiment. As listed in Table 4, for all the tested catalysts both the NO consumption and N$_2$ production match reasonably well (experimental error within +/- 10%) the overall number of Cu ions present in the sample measured by ICP-MS (Table 1), indicating that all the Cu in the tested samples is indeed reducible, regardless of SAR and Cu loading. It is worth mentioning that the values listed in Table 4 are due to two contributions. Indeed, in the NO+NH$_3$ TPR test the catalysts were exposed to NO first and to NH$_3$ then at the minimum test temperature (80°C). Only when both signals were stable, the T-ramp was

13

started. This protocol was chosen to observe in the most accurate way the NO consumption and the N_2 production. However, for all samples we observed a preliminary 1:1 NO consumption and N_2 production during the isothermal co-feed of NO and NH_3 at 80°C. During the T-ramp, the rest of Cu sites were reduced: the sum of these two contributions match quite well the total amount of Cu sites present in each catalyst. In the case of the 0.7% Cu sample, which contains a substantially lower amount of Cu ions with respect to the other samples, the intensity of the peak observed during the T-ramp is much smaller with respect to the other samples, bacause the isothermal reduction strongly reduced the peak intensity of the following TPR part of the test.

Table 4. NO consumption and N_2 production from NO+NH_3 – TPR experiments

	Cu/Al [-]	SAR [-]	Cu tot [μmol]	NO consumption [μmol]	N_2 production [μmol]
1.7Cu-CHA10	0.12	10	4.3	3.9	4.4
1.7Cu-CHA13	0.17	13	4.3	4.5	4.0
1.7Cu-CHA17	0.21	17	4.3	3.9	4.5
1.7Cu-CHA22	0.24	22	4.3	3.9	4.0
0.7Cu-CHA25	0.11	25	1.8	1.6	1.9
1.7Cu-CHA25	0.24	25	4.3	3.9	4.3
2.1Cu-CHA25	0.29	25	5.2	4.9	5.8

The NO + NH_3 TPR results are therefore in line with the H_2-TPR runs, confirming the different reducibility of the two Cu species in Cu-CHA. Moreover, this simple characterization technique could be useful to estimate in a simple way the amount of all reducible Cu ions contained in a Cu-CHA catalyst. However, the individual estimation of each type of Cu ion ($ZCu^{II}OH$ versus Z_2Cu^{II}) is not possible due to their similar reduction behavior in presence of this reducing agent. Gaseous NH_3 in fact results in full saturation of both types of Cu ions in the form of $[Cu(NH_3)_4]^{2+}$ and $[Cu(OH)(NH_3)_3]^+$, which become completely detached from the zeolite framework as mobile species [11, 20]. Therefore, ammonia ligands seem to play a crucial role in the Cu reduction route, since they confer mobility to the Cu species changing substantially the reduction behavior observed when using only H_2 (Figure 1). Moreover, this test emphasizes how facile the Cu reduction is under conditions

close to those of the SCR process: the adoption of NH_3+NO (Figure 2 and 3) instead of H_2 as reducing agent (Figure 1) shifts all the reduction temperatures to much lower values, in a useful range for the purposes of NO_x abatement.

3.3 NO_2 adsorption + TPD

NO_2 adsorption - desorption runs were performed with the purpose of investigating formation and stability of nitrates on the catalysts samples with different Cu loadings and SAR. Figures 4A and 5A illustrate the Cu loading effect and the SAR effect, respectively, on the dynamic evolutions of NO_2 and NO observed during the adsorption phase of NO_2 at 120 °C. All the catalysts exhibit the same initial behavior governed by a well-known chemistry, with NO_2 adsorption combined with a simultaneous fast NO release associated with the disproportionation of NO_2 and the formation of surface nitrates [6,23]. After reaching saturation, the NO_2 feed was switched off in order to desorb, firstly, the weakly bound NOx species and, finally, the chemisorbed ones upon the linear T-increase (TPD phase in Figures 4B and 5B for the Cu loading and SAR effect, respectively). Table 5 reports the quantitative analysis of the NO_2 TPD runs, computed by integration of the NO_x inlet and outlet temporal profiles.

Some considerations can be made starting from the Cu loading effect. The bare zeolite is not able to store NO_2, in fact the amount of chemisorbed NO_x species is negligible. As the Cu content of the Cu-CHA samples increases, a clear increment in the amount of stored species is observed, quite significant when comparing the TPD profiles in Figure 4B. From this result, we can first conclude that the storage of nitrates occurs on Cu ions[6,24–26]. In fact, the amount of stored nitrates, being linked to the number of Cu ions, is boosted considerably on increasing the Cu loading, reaching the highest value (218 μmol/g) over the 2.1% Cu-CHA sample.
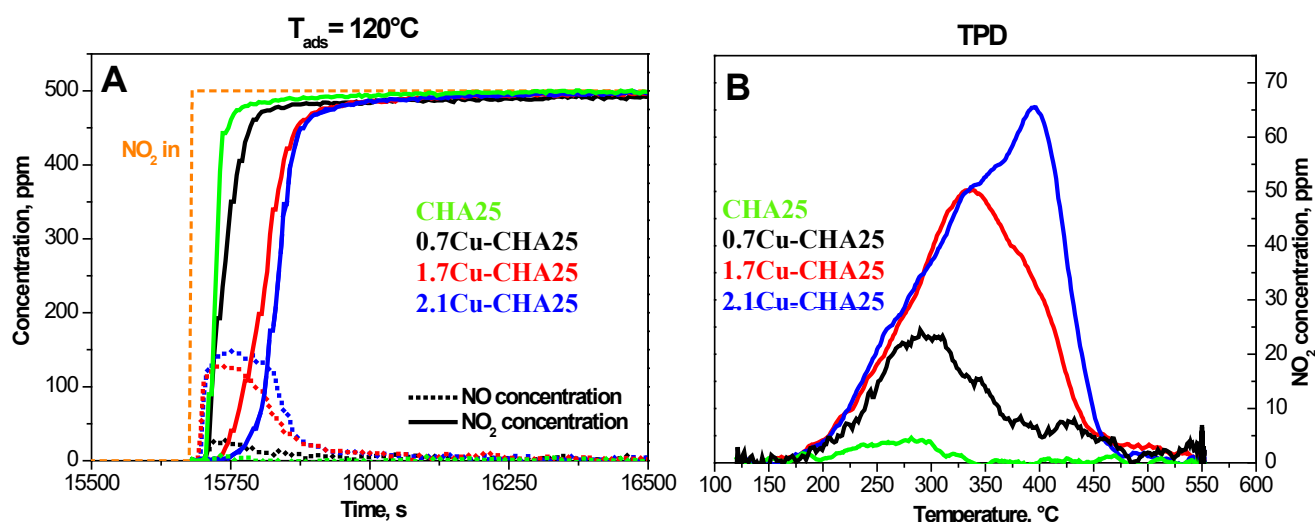
Figure 4. Cu-CHA catalysts with SAR=25 and different Cu loadings (0-3 % w/w). A) NO_2 adsorption dynamics at 120 °C, NO_2= 500 ppm, H_2O= 0% v/v; B) TPD after NO_2 adsorption at 120 °C, heating rate= 15 °C/min, He. GHSV= 450000 cm^3/(g$_{cat}$*h) STP. Pre-oxidized catalysts.

We notice however that samples with the same Cu loading (1.7 % w/w) but with higher SAR were associated with a greater storage capacity of nitrates (up to about 154 μmol/g for 1.7Cu-CHA25). This suggests that the storage of nitrates is controlled not only by the overall Cu loading. Moreover, even if less pronounced, a shift of the NO_2 peak towards higher temperatures was noted when moving to higher SAR.
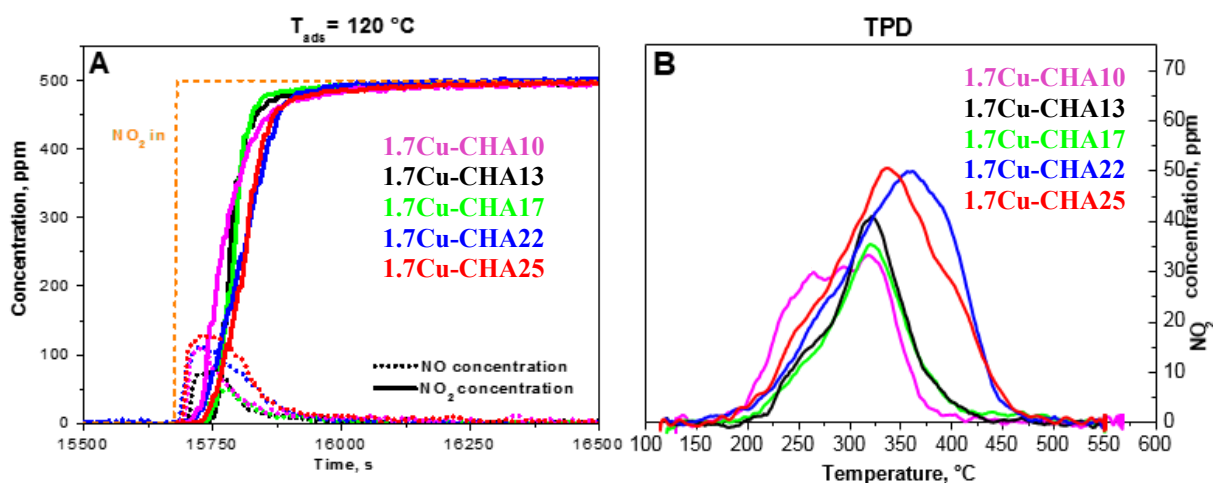

Figure 5. Cu-CHA catalysts with Cu loading= 1.7% w/w and different SARs (10, 13, 17, 22, 25). A) NO_2 adsorption dynamics at 120 °C, NO_2= 500 ppm, H_2O= 0% v/v; B) TPD after NO_2 adsorption at 120 °C, heating rate= 15 °C/min, He. GHSV= 450000 cm^3/(g$_{cat}$*h) STP. Pre-oxidized catalysts.

Table 5. Cu loading and SAR effects on NO_2 storage.

	Cu loading effect				SAR effect				
	0%	0.7%	1.7%	2.1%	10	13	17	22	25
NO$_2$ adsorbed (µmol)	2.5	3.7	5.3	6.1	4.0	4.7	4.6	4.6	5.3
NO$_2$ physisorbed (µmol)	1.7	2.1	2.0	1.8	2.4	3.1	3.2	2.0	2.0
NO$_2$ chemisorbed (µmol)	0.1	1.2	2.5	3.5	1.9	1.2	1.2	2.5	2.5
N-balance error (%)	27	11	15	13	9	9.0	5.0	3.0	15

Jangjou et al. [18] studied the responses of Cu-CHA catalysts with different fractions of $ZCu^{II}OH$ sites towards SO_2 exposure. They observed that Z_2Cu^{II} sites adsorbed SO_2 only when co-feeding ammonia; on the contrary, SO_2 alone was able to interact readily with $ZCu^{II}OH$ sites only. Furthermore, the higher the fraction of $ZCu^{II}OH$ sites in Cu-CHA, the higher was the required desulfation temperature. In analogy to SO_2, quantitative evidence about the Cu speciation can be inferred by looking at the NO_2 adsorption. Assuming that only $ZCu^{II}OH$ sites can store nitrates, as also recently demonstrated through spectroscopic techniques by Negri et al. [27], the NO_2 storage mechanism can be written as follows[24]

$$2ZCu^{II}OH + 3NO_2 \rightarrow 2ZCu^{II}NO_3 + NO + H_2O \qquad (6)$$

Therefore, the integral amount of NO released during the NO_2 adsorption can be used to quantify the $ZCu^{II}OH$ sites in the catalyst sample, according to the stoichiometry of reaction (6) ($ZCu^{II}OH/NO=2/1$). Moreover, also the NO_2 released during the following TPD phase is directly linked to the amount of $ZCu^{II}OH$, since each hydroxylated Cu ion can store one nitrate species, whose decomposition releases one NO_2 molecule ($ZCu^{II}OH/NO_2=1/1$). The last two columns of Table 6 show in fact that the fractions of $ZCu^{II}OH$ sites estimated from the H_2-TPR data on the 1.7Cu-CHA10, 0.7Cu-CHA25 and 2.1Cu-CHA25 samples (Table 3) and those computed from both the NO release and the NO_2-TPD during the NO_2 adsorption runs match reasonably well.

Table 6. $ZCu^{II}OH$ estimated from the H_2-TPR results and from the NO_2 ads/TPD tests

Sample	Cu tot [μmol]	ZCu^{II}OH from H$_2$-TPR results [μmol]	% ZCu^{II}OH from NO$_2$ ads/TPD results			
			NO released [μmol]	NO$_2$ TPD [μmol]	NO$_2$ TPD/ ZCu^{II}OH [μmol/ μmol]	2*NO released /ZCu^{II}OH [μmol/ μmol]
1.7Cu-CHA10	4.3	2.4	1.2	2.0	0.8	1.0
0.7Cu-CHA25	1.8	1.0	0.5	1.2	1.2	1.0
2.1Cu-CHA25	5.2	4.1	2.1	3.5	0.9	1.0

Moreover, a NO$_2$ storage mechanism which involves only ZCu^{II}OH sites can well explain why catalysts characterized by the same Cu loading but with different SAR showed an increased NO$_2$ storage capacity. Indeed, to Cu-CHA with higher SAR correspond catalysts with higher ZCu^{II}OH fractions which can accordingly accommodate more stored nitrates.

In addition to the storage capacity, SAR and Cu loading affect also the stability of the stored nitrates. Indeed, observing the position of the temperature peaks of the different TPD profiles a further consideration can be made: the samples with higher presence of ZCu^{II}OH ions are characterized by TPD with peaks centered at higher temperatures and thus by more stable stored nitrates, which is consistent with the corresponding greater stability of sulfates according to the literature [18]. Yuvaraj et al. [28] proposed that the decomposition temperatures of different metal nitrates are inversely correlated to the charge densities of the metal cations. When the metal ion has a high electro-positivity, it is able to strongly attract one of the oxygens in the nitrate group, weakening the N-O bond and, consequentially, facilitating its opening. This finding might explain why we observe a progressive enhancement in the nitrate stability when the Cu loading increases. Changing the Cu/Al ratio means changing the Al distribution within the CHA cages. This different Al distribution might affect the charge density on the ZCu^{II}OH sites and consequently the stability of adsorbed species on these sites and, correspondingly, the temperature required for their thermal decomposition.

In more general terms, the present NO$_2$ adsorption + TPD tests have revealed another simple characterization technique which can not only validate the existence of two populations of Cu cations

in Cu-CHA, but most of all can be used to directly quantify their proportions, thanks to quite different behaviors in the storage of NO_2/nitrates.

3.4 NH_3 adsorption + TPD

Finally, we use the NH_3 adsorption + TPD test to characterize the interaction between the NOx reducing agent of the SCR process, NH_3, and the Cu-CHA catalysts. Through this test it is possible not only to estimate the overall NH_3 storage capacity of the catalyst but also to titrate different acid sites present in the metal-promoted zeolite. We performed all the adsorption tests under dry conditions in order to avoid the complexities associated with the presence of water (e.g. competitive adsorption between NH_3 and H_2O on active sites), even if water is of course always present in the reaction environment in real SCR applications. The effect of H_2O on Cu-speciation in Cu-CHA will be studied in detail in a distinct dedicated work.

Like the NO_2 adsorption + TPD runs, the tests included the three stages described in the Experimental Section 2.2. The adsorption and TPD plots of all the investigated catalysts are presented in Figure 6 (Cu loading effect) and Figure 7 (SAR effect).

Starting with the Cu loading effect, Figure 6A illustrates the NH_3 dynamics during the adsorption phase at 150 °C. All the catalysts showed a dead time, i.e. an interval in which the ammonia fed to the reactor is completely adsorbed onto the catalyst and no ammonia molecules reach the analyzer. The dead time is proportional to the number of the acid sites in the catalyst: indeed, it increased from 530 s over the un-promoted zeolite to 860 s over the sample with the highest Cu loading. After the dead time, the ammonia outlet concentration increased and gradually approached the feed concentration level upon catalyst saturation.

To understand more about the nature of the active sites involved in the SCR reactions we focused on the TPD, when the chemisorbed ammonia is eventually released (Figure 6B). The bare zeolite (green curve) is characterized by one single NH_3-peak centered at 440 °C and assigned to NH_3 adsorbed as NH_4^+ on Brønsted sites[29–31]. The unpromoted zeolite shows also a weak shoulder at lower

19

temperature related to the presence of extra-framework aluminum atoms which provide a slight Lewis acidity[29–32], confirmed by the Al solid state MAS NMR experiments.

When the catalysts are promoted with Cu ions, another NH_3 desorption peak centered at lower temperature (300 °C) becomes apparent. It can be therefore associated with the Cu ions, which increase the Lewis acidity of the catalyst [29–32]. Expectedly, the intensity of this peak grows on increasing the Cu loading, there being more sites available for the adsorption of NH_3. Moreover, a drop in the Brønsted peak is appreciable as the Cu content is increased: in fact, when the zeolite structure is exchanged with Cu ions, more Lewis acid sites are created via occupation of Brønsted acid sites [8] and this justifies the decrement of the high-T Brønsted NH_3 desorption peak with increasing Cu loading. The overall (Lewis + Brønsted) storage capacity of Cu-CHA is slightly enhanced by the presence of more Cu ions in the catalyst. Table 7 presents the quantitative analysis of the whole set of tests, computed via the integration of the NH_3 inlet and outlet temporal profiles.
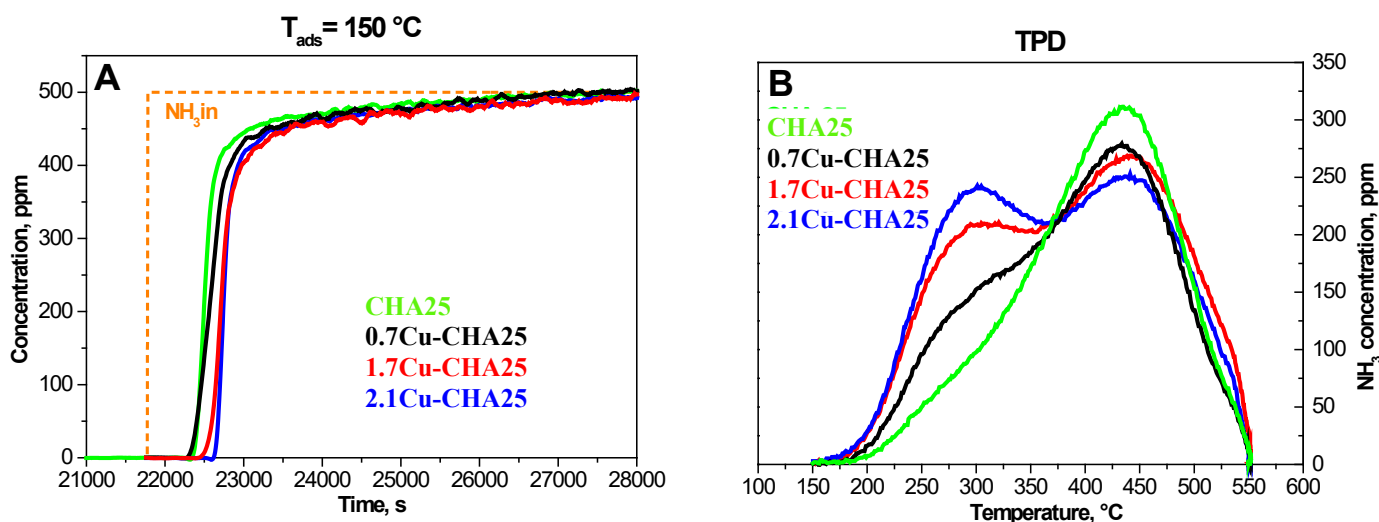

Figure 6. Comparison of Cu-CHA catalysts with SAR=25 and different Cu loadings (0-3 % w/w). A) NH_3 adsorption phase dynamics at 150 °C, NH_3= 500 ppm, H_2O= 0% v/v; B) TPD after NH_3 adsorption at 150 °C, heating rate= 15 °C/min, He. GHSV= 266250 $cm^3/(g_{cat}$*h) STP. Pre-oxidized catalysts.

The same test was carried out over the second set of Cu-CHA catalysts characterized by constant Cu content (1.7% w/w) and different SiO_2/Al_2O_3 ratios. The data collected during the NH_3 adsorption phase and during the TPD phase are shown in Figure 7A and Figure 7B, respectively.

Looking at Figure 7A, all the catalysts showed a similar dead time of about 850 s and quite similar dynamics. Moreover, all the research samples were promoted with the same Cu amount and therefore, as expected, all the TPD curves were characterized by a bimodal desorption profile (Figure 7B): the first peak is ascribed to the NH_3 adsorbed onto Cu ions (plus a fraction of Al extra-framework detected from Al solid state MAS NMR experiments) and the second one is associated with the Brønsted sites of the zeolite framework.

The SAR effect on the NH_3 storage is also quite evident: increasing the SiO_2/Al_2O_3 ratio increases the stability of the stored ammonia, so that the amount of NH_3 released by the weaker sites decreases, while that stored on the Brønsted sites increases (Figure 7A). Although the proportion between Lewis ammonia and Brønsted ammonia changes notably upon varying SAR, the overall amount of chemisorbed NH_3 does not change, as shown by the similar values reported in Table 6. The SAR of the studied catalysts varies only between 10 and 25, which therefore corresponds to similar Bronsted acidity (confirmed by NH_3-TPD experiments on the corresponding bare zeolites). When the catalysts were promoted with Cu ions, part of the Bronsted acid sites were converted into Lewis acid sites due to the exchange of the protons with Cu ions. At low SAR (high aluminum content), Cu ions were mostly exchanged as Z_2Cu^{II} and thus for each Cu ions two Brønsted sites were lost. On the contrary, at high SAR, Cu ions were more likely present as $ZCu^{II}OH$ sites: for each Cu ion, only one Bronsted site was lost in this case. However, Z_2Cu^{II} sites are able to coordinate a greater number of NH_3 molecules than $ZCu^{II}OH$. Consequentially, on increasing SAR the intensity of the low-T TPD peak (Lewis acidity) decreased while the high-T peak (Brønsted sites) was enhanced. These different contributions to the NH_3 storage could explain why we did not observe a change in the amount of the chemisorbed NH_3 but only an evident different distribution of NH_3 on the acid sites when SAR was varied. The differences in the NH_3 coordination to Cu sites when changing SAR or Cu loading are further discussed below.
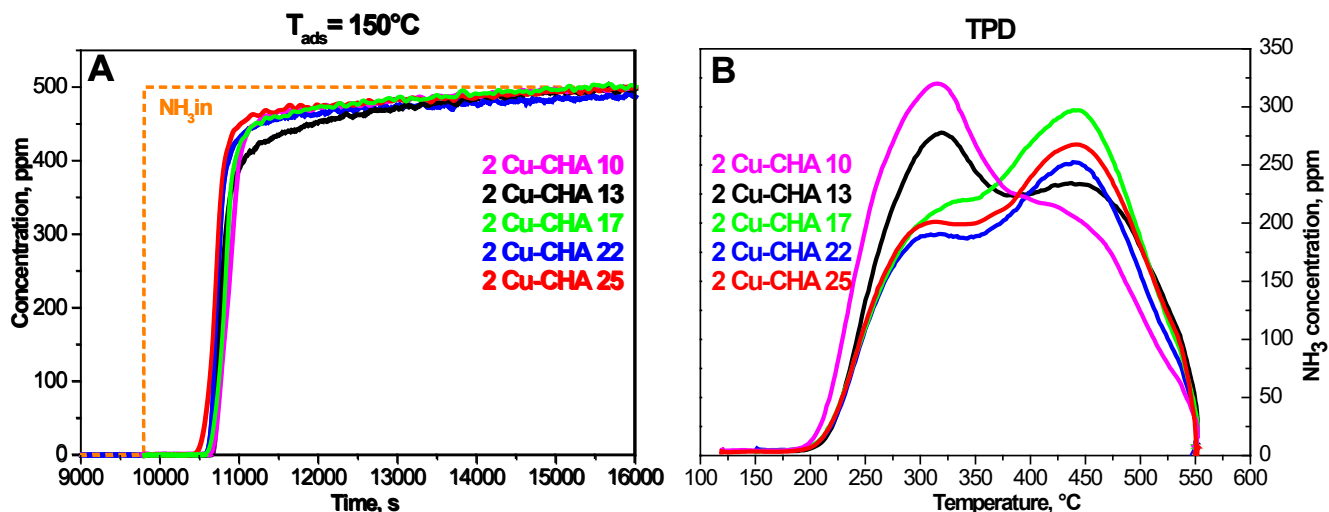
1.7Cu-CHA10
1.7Cu-CHA13
1.7Cu-CHA17
1.7Cu-CHA22

Figure 7. Comparison among Cu-CHA catalysts with Cu loading= 1.7% w/w and different SARs (10, 13, 17, 22, 25). A) NH_3 adsorption phase dynamics at 150 °C, NH_3= 500 ppm, H_2O= 0% v/v; B) TPD after NH_3 adsorption at 150 °C, heating rate= 15 °C/min, He. GHSV= 266250 $cm^3/(g_{cat}*h)$ STP. Pre-oxidized catalysts.

Table 7. Cu loading and SAR effects on NH_3 adsorption

	Cu loading effect				SAR effect				
	0%	0.7%	1.7%	2.1%	10	13	17	22	25
NH_3 adsorbed (µmol)	18.7	18.9	23.4	24.7	25.2	33.3	30.1	31.2	23.4
NH_3 physisorbed (µmol)	5.7	6.7	10.0	9.2	9.4	9.9	9.5	9.0	10.0
NH_3 chemisorbed (µmol)	11.9	12.2	14.5	14.2	14.9	16.3	16.0	14.4	14.5
N-balance error (%)	6	1	8	5	4	21	15	24	8

The existence of two populations of Cu cations affects the NH_3 storage capacity of the Cu-CHA catalyst. Paolucci et al. [11] found that the two Cu sites differ in their NH_3 coordination behaviour: they observed that the hydroxylated Cu site ($ZCu^{II}OH$) is able to coordinate and store 3 ammonia molecules, while the doubly bound Cu site (Z_2Cu^{II}) can store up to 4 ammonia molecules, according to the following stoichiometries:

$$4NH_3 + Cu^{II} \rightarrow Cu^{II}(NH_3)_4 \tag{7}$$

$$3NH_3 + Cu^{II}OH \rightarrow Cu^{II}(OH)(NH_3)_3 \tag{8}$$
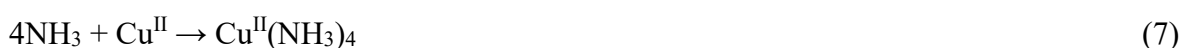
As already shown in literature [9,11,12,18,20], and as seen also from our H_2-TPR and NO_2-TPD data, the fraction of $ZCu^{II}OH$ increases with increasing Si/Al and/or Cu/Al ratios and accordingly also the amount of NH_3 coordinated to the Cu ions is affected. Therefore, also the NH_3-TPD could be used to probe experimentally the Cu speciation.

We thus calculated the NH_3/Cu ratio as an index for the impact of Cu loading and SAR on Cu speciation. For the evaluation of this ratio, only the NH_3 bound to Cu ions has to be considered. Since NH_3 can be stored on three types of sites, namely Al extra-framework, Cu sites, Brønsted sites, the NH_3 stored on Cu ions only was quantified through a Gaussian deconvolution that takes into account the three storage acid sites, through which we obtained the best fit of the NH_3-TPD profiles. Examples of TPD deconvolutions are shown in Figure 8. It is worth mentioning here that the amount of extra-framework Al was first evaluated through the deconvolution of the NH_3-TPD of the bare zeolites with different SAR and then kept constant for all the Cu exchanged catalysts. All zeolites contained significant levels of extra-framework Al and their amounts decreased with increasing SAR[32], as observed through the ^{27}Al solid-state MAS NMR spectra.
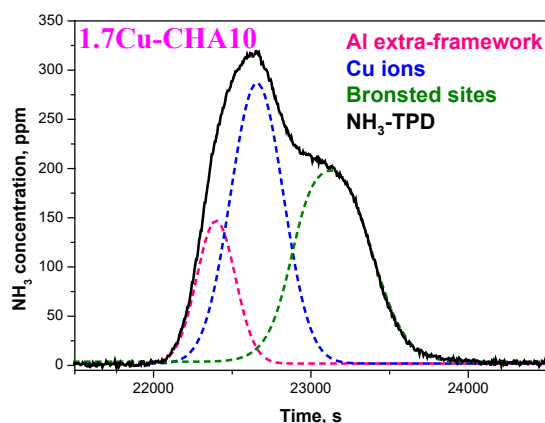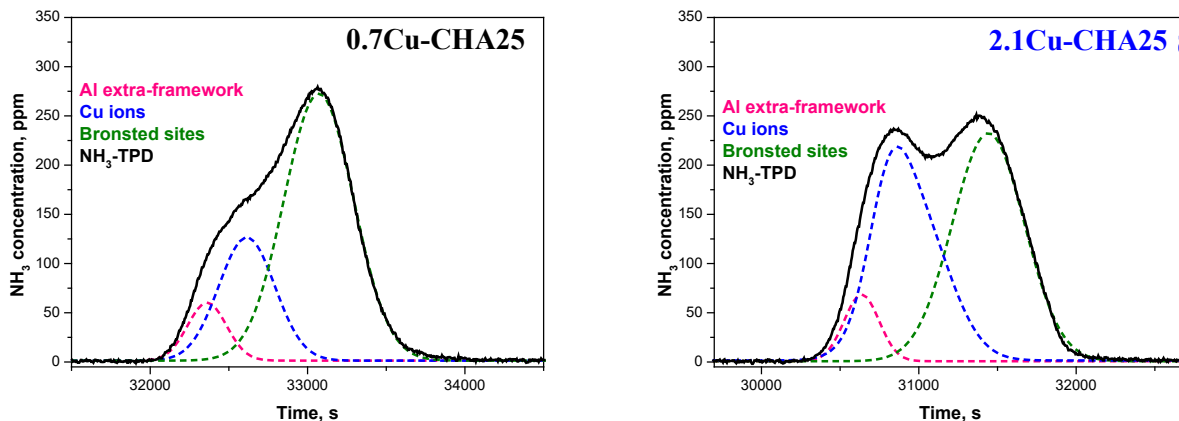
Figure 8. Deconvolution of the NH_3-TPD profiles: evaluation of NH_3 stored on Al extra-framework, Cu ions and Bronsted sites.

Table 8 lists the three contributions to the NH_3 TPD curves for all the Cu-CHA samples as estimated from the deconvolution of the NH_3-TPD curves.

Table 8. NH_3 adsorbed on different sites as estimated from NH_3-TPD deconvolution

	Cu/Al	NH_3 - Al extra-framework [µmol]	NH_3 -Cu [µmol]	NH_3 Brønsted [µmol]	NH_3-TPD [µmol]
1.7Cu-CHA10	0.12	2.5	6.5	6.2	14.9
1.7Cu-CHA13	0.17	2.0	5.4	8.3	16.3
1.7Cu-CHA17	0.21	1.9	5.2	8.4	16.0
1.7Cu-CHA22	0.24	1.7	5.1	8.0	14.4
0.7Cu-CHA25	0.11	1.1	3.0	8.0	12.2
1.7Cu-CHA25	0.24	1.2	5.4	7.9	14.5
2.1Cu-CHA25	0.29	1.1	6.1	6.7	14.1

Once the amount of NH_3 stored on Cu ions only was known, the number of NH_3 molecules coordinated by each Cu atom was computed. Figure 9 illustrates how this ratio varies with the Cu/Al ratio. From theory [11] we expect a decreasing trend of the NH_3/Cu ratio when Cu/Al increases, since the fraction of $ZCu^{II}OH$ increases and these sites coordinate less NH_3 than Z_2Cu^{II}. The ratio evaluated from our data falls in the range 1-2 (curve in the blue zone of Figure 9) and, although this range is quite far from the one proposed by Paolucci et al. (3-4) [11], the observed trend is in line with the

theoretical expectations and with other literature findings: the NH_3/Cu ratio decreases on moving towards both higher SAR and higher Cu loading (i.e. towards higher Cu/Al). However, Luo et al. [9], from similar considerations made on Cu-CHA catalysts subjected to aging treatment that leads to a progressive transition from $ZCu^{II}OH$ to Z_2Cu^{II}, estimated the range 1-2 for their NH_3/Cu ratios, which is quantitatively in line with our results. The difference between the two proposed ranges (3-4 vs. 1-2) is likely connected to the conditions adopted during the test. When NH_3 is present in the gas phase the full saturation of Cu ions occurs, achieving the 3-4 range proposed by Paolucci et al. [11]. Under these conditions, indeed, Cu ions are completely detached from the zeolite and can coordinate the maximum number of ammonia molecules [9,11]. Therefore, the NH_3/Cu calculations were repeated adding the amount of NH_3 ligated to Cu ions (from the TPD) to the NH_3 released during the isothermal physi-desorption phase, so taking into account all the NH_3 coordinated to the catalyst when it is fully saturated. The physisorbed NH_3 represents in fact the additional ammonia molecules that are coordinated to Cu ions when ammonia is in the gas phase and solvates the Cu sites. Taking into account the physisorbed NH_3, the NH_3/Cu ratio increases and falls in the theoretical range 3-4 within experimental error (yellow zone in Figure 9). The values used for the estimation of the NH_3/Cu ratios (i.e. Cu tot, NH_3/Cu, physisorbed NH_3) are listed in Table 9.
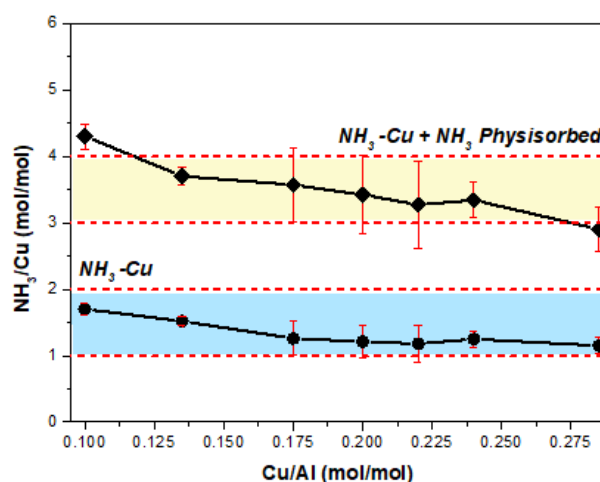

Figure 9. NH_3/Cu ratios vs. Cu/Al: comparison between NH_3/Cu ratios evaluated considering only NH_3 stored on Cu ions (low-T peak of TPD) and NH_3 stored on Cu ions plus NH_3 physisorbed.

Table 9. NH$_3$/Cu ratios estimated from the NH$_3$-TPD deconvolution.

[†] NH$_3$/Cu ratio considering the NH$_3$ on Cu sites (intermediate peak shown in Figure 4);

[††] NH$_3$/Cu ratio considering the NH$_3$ on Cu sites (intermediate peak shown in Figure 4) + physisorbed NH$_3$.

	Cu/Al [-]	Cu tot [μmol]	NH$_3$−Cu (int-T peak dec) [μmol]	NH$_3$/Cu [†] [-]	NH$_3$ physisorbed [μmol]	NH$_3$/Cu [††] [-]
1.7Cu-CHA10	0.12	4.3	6.5	1.5	9.5	3.70
1.7Cu-CHA13	0.17	4.3	5.4	1.3	9.9	3.57
1.7Cu-CHA17	0.21	4.3	5.2	1.2	9.5	3.42
1.7Cu-CHA22	0.24	4.3	5.1	1.2	9.0	3.27
0.7Cu-CHA25	0.11	1.8	3.0	1.6	4.3	4.33
1.7Cu-CHA25	0.24	4.3	5.4	1.3	10.0	3.51
2.1Cu-CHA25	0.29	5.2	6.1	1.2	9.3	2.90

Remarkably, the NH$_3$/Cu ratios extracted from the deconvolution of the TPD plots are quite in good agreement with theoretical estimates based on the number of Z$_2$Cu^{II} and ZCu^{II}OH sites from the H$_2$-TPR (Table 2) and on the number of NH$_3$ molecules coordinated to each one of the two Cu species according to the NH$_3$ adsorption stoichiometries proposed in literature [9,11]. Table 10 compares the NH$_3$/Cu ratios calculated from the H$_2$-TPR data and from the NH$_3$-TPD deconvolution. The NH$_3$/Cu estimates determined with both techniques match fairly well, suggesting the adequacy of both experimental methods to probe the Cu speciation, particularly for the stoichiometry of Luo et al. [9] (1-2 range).

Table 10. NH$_3$/Cu ratios estimated from the H$_2$-TPR results and from the NH$_3$-TPD deconvolution.

[*] NH$_3$/Cu ratio considering 2 NH$_3$ for Z$_2$Cu^{II} and 1 NH$_3$ for ZCu^{II}OH [9];

[**] NH$_3$/Cu ratio considering 4 NH$_3$ for Z$_2$Cu^{II} and 3 NH$_3$ for ZCu^{II}OH [11];

[†] NH$_3$/Cu ratio considering the NH$_3$ on Cu sites (intermediate peak in Figure 4);

[††] NH$_3$/Cu ratio considering the NH$_3$ on Cu sites (intermediate peak in Figure 4) + physisorbed NH$_3$.

Sample	Cu tot [μmol]	NH$_3$/Cu ratios estimated from H$_2$-TPR results				NH$_3$/Cu ratios estimated from NH$_3$-TPD deconvolution	
		Z$_2$Cu^{II} [μmol]	ZCu^{II}OH [μmol]	NH$_3$/Cu* [-]	NH$_3$/Cu** [-]	NH$_3$/Cu [†] [-]	NH$_3$/Cu [††] [-]
1.7Cu-CHA10	4.3	1.9 (44%)	2.4 (56%)	1.4	3.4	1.5	3.7
0.7Cu-CHA25	1.8	0.8 (45%)	1.0 (55%)	1.5	3.5	1.6	4.3
2.1Cu-CHA25	5.2	1.0 (21%)	4.2 (79%)	1.2	3.2	1.2	2.9

4   Conclusions

The effects of SAR and Cu loading on the Cu speciation were studied on two sets of Cu-CHA model catalysts. Four characterization tests, namely H_2-TPR, NO+NH_3-TPR, NO_2 adsorption + TPD and NH_3 adsorption + TPD, were carried out in order to evaluate how the two catalyst formulation parameters affect the nature of the Cu active centers, their interaction with NH_3, NO and NO_2 and their reducibility. In addition, these tests demonstrated the potential of experimentally probing the reducible Cu-sites and their speciation (i.e. $ZCu^{II}OH$ versus Z_2Cu^{II}) in Cu-CHA using simple transient techniques.

The H_2-TPR experiments provided preliminary indications on how the relative amounts of the two populations of Cu species change in our model catalysts on varying SAR and Cu loading, as already applied in literature studies.

The NO+NH_3-TPR tests proved to be a convenient method to titrate all the reducible Cu in Cu-CHA: in fact, one NO molecule is consumed and one N_2 molecule is produced for each reduced Cu ion, so by looking at the integral NO consumption and N_2 release we could show that about 100% of Cu was reducible in our samples. Also, Cu-CHA samples with lower Cu loading or lower SAR show reduction peaks centered at lower temperature, meaning that they contain higher fractions of Z_2Cu^{II} sites, which are less reducible, in line with the H_2-TPR tests.

The NO_2 adsorption-TPD runs demonstrated that nitrate species are stored only on $ZCu^{II}OH$ species, which explains the positive effects on the amounts of stored nitrates observed when increasing both SAR and Cu content. Accordingly, this simple technique is proposed as the preferred method for direct quantification of the fraction of $ZCu^{II}OH$ in Cu-CHA. In fact, the NO released during the NO_2 adsorption phase is linked to the $ZCu^{II}OH$ species through the $ZCu^{II}OH/NO=2/1$ stoichiometry. In the same way, also the integral of NO_2 released during the TPD phase can be used to estimate the fraction of $ZCu^{II}OH$, in this case according to a 1/1 ratio resulting from nitrates decomposition.

Finally, the ammonia adsorption-TPD runs evidenced that the higher the Cu loading and the SiO$_2$/Al$_2$O$_3$ ratio, the lower is the Lewis acidity of the Cu-CHA catalysts, and consequently the lower is the number of NH$_3$ molecules coordinated by each Cu atom, due to a corresponding increase of the fraction of ZCu^{II}OH, which ligates three NH$_3$ molecules against the four NH$_3$ molecules coordinated by Z$_2$Cu^{II} sites. Analysis of the NH$_3$-TPD curves, based on their deconvolution to isolate the Lewis NH$_3$, provided estimates of the fraction of ZCu^{II}OH species in line with those obtained from H$_2$-TPR runs. Therefore, NH$_3$ adsorption-TPD represents a possible alternative method of probing Cu speciation in Cu-CHA. It is however more complicated than NO$_2$ adsorption-TPD as it requires deconvolution of the NH$_3$-TPD curves.

Altogether, the simple transient response methods applied in this work to probe the Cu speciation in Cu-CHA catalysts have provided converging results, which not only point out the different characteristics of the two prevailing Cu cations, but also enable a straightforward quantitative determination of their relative proportions.

References

1. Nova, I.; Tronconi, E. Urea-SCR technology for deNOx after treatment of Diesel Exhaust. (Springer, 2014).

2. Gao, F.; Kwak, J.H.; Szanyi, J.; Peden, C.H.F., Current Understanding of Cu-Exchanged Chabazite Molecular Sieves for Use as Commercial Diesel Engine DeNOx Catalysts. Topics in Catalysis 2013, 56, 1441–1459.

3. Wang, J.; Zhao, H.; Haller, G.L.Y., Recent advances in the selective catalytic reduction of

NO_x with NH_3 on Cu-Chabazite catalysts. Appliedd Cataysis B: Environmental 2017, 202, 346–354.

4.   Fickel, D.W.; D'Addio, E.; Lauterbach, J.A.; Lobo, R. F., The ammonia selective catalytic reduction activity of copper-exchanged small-pore zeolites. Applied Cataysis B: Environmental 2011, 102, 441–448.

5.   Beale, A.M.; Gao, F.; Lezcano-Gonzalez, I.; Peden, C.H.F.; Szanyi, J., Recent advances in automotive catalysis for NO_x emission control by small-pore microporous materials. Chemical Society Review 2015, 44, 7371–7405.

6.   Ruggeri, M.P.; Nova, I.; Tronconi, E.; Collier, J.E.; York, A.P.E., Structure–Activity Relationship of Different Cu–Zeolite Catalysts for NH_3–SCR. Topics in Catalysis 2016, 59, 875–881.

7.   Fan, C.; Chen, L.; Pang, L.; Ming, S.; Zhang, X; Albert, K.B.; Liu, P.; Chen, H.; Li, T., The influence of Si/Al ratio on the catalytic property and hydrothermal stability of Cu-SSZ-13 catalysts for NH3-SCR. Applied Catalysis A: General 2018, 550, 256–265.

8.   Wang, D.; Zhang, L.; Li, J.; Kamasamudram, K.; Epling, W.S., NH3-SCR over Cu/SAPO-34 – Zeolite acidity and Cu structure changes as a function of Cu loading. Catalysis Today 2014, 231, 64–74.

9.   Luo, J.; Gao, F.; Kamasamudram, K.; Currier, N.; Peden, C.H.F.; Yezerets, A., New insights into Cu/SSZ-13 SCR catalyst acidity. Part I: Nature of acidic sites probed by NH3 titration. Journal of Catalysis 2017, 348, 291–299.

10.   Song, J.; Wang, Y.; Walter, E.D.; Washton, N.M.; Mei, D.; Kovarik, L.; Engelhard, M.H.; Prodinger, S.; Wang, Y.; Peden, C.H.F.; Gao, F., Toward Rational Design of Cu/SSZ-13 Selective Catalytic Reduction Catalysts: Implications from Atomic-Level Understanding of Hydrothermal Stability. ACS Catalysis 2017, 7, 8214–8227.

11.   Paolucci, C. Parekh, A.A.; Khurana, I.; Di Iorio, J.R.; Li, H.; Albarracin Caballero, J.D.; Shih, A.J.; Anggara, T.; Delgass, W.N.; Miller, J.T.; Ribeiro, F.H.; Gounder, R.; Schneider,

W.F., Catalysis in a cage: Condition-dependent speciation and dynamics of exchanged cu cations in SSZ-13 zeolites. Journal of the American Chemical Socieety 2016, 138, 6028–6048.

12. Gao, F.; Washton, N.M.; Wang, Y.; Kollar, M.; Szanyi, J.; Peden, C.H.F., Effects of Si/Al ratio on Cu/SSZ-13 NH_3-SCR catalysts: Implications for the active Cu species and the roles of Brønsted acidity. Journal of Catalysis 2015, 331, 25–38.

13. Hun Kwak, J.; Zhu, H.; Lee, J. H.; Peden, C.H.F.; Szanyi, J., Two different cationic positions in Cu-SSZ-13? Chemical Communications 2012, 48, 4758–4760.

14. Andersen, C.W.; Bremholm, M.; Vannestrom, P.N.R.; Blichfeld, A.B.; Lundegaard, L.F.; Iversen, B.B., Location of Cu^{2+} in CHA zeolite investigated by X-ray diffraction using the Rietveld/maximum entropy method. IUCr Journal 2014, 1, 382–386.

15. Fickel, D.W.; Lobo, R.F., Copper coordination in Cu-SSZ-13 and Cu-SSZ-16 investigated by variable-temperature XRD. Journal of Physical Chemistry C 2010, 114, 1633–1640.

16. Kwak, J.H.; Varga, T.; Peden, C.H.F.; Gao, F.; Hanson, J.C.; Szanyi, J., Following the movement of Cu ions in a SSZ-13 zeolite during dehydration, reduction and adsorption: A combined in situ TP-XRD, XANES/DRIFTS study. Journal of Catalysis 2014, 314, 83–93.

17. Martini, A.; Borfecchia, E.; Lomachenko, A.; Pankin, I.A.; Negri, C.; Berlier, G.; Beato, P.; Falsig, H.; Bordiga, S.; Lamberti, C., Composition-driven Cu-speciation and reducibility in Cu-CHA zeolite catalysts: A multivariate XAS/FTIR approach to complexity. Chemical Science 2017, 8, 6836–6851.

18. Jangjou, Y.; Do, Q.; Gu, Y.; Lim, L.; Sun, H.; Wang, D.; Kumar, A.; Li, J.; Grabow, L.C.; Epling, W.S., Nature of Cu Active Centers in Cu-SSZ-13 and Their Responses to SO_2 Exposure. Journal of the American Chemical Society 2018, 8, 1325–1337.

19. Gao, F.; Walter, E.D.; Kollar, M.; Wang, Y.; Szanyi, J.; Peden, C.H.F., Understanding ammonia selective catalytic reduction kinetics over Cu/SSZ-13 from motion of the Cu ions. Journal of Catalysis 2014, 319, 1–14.

20. Gao, F.; Peden, C. H. F., Recent Progress in Atomic-Level Understanding of Cu/SSZ-13 Selective Catalytic Reduction Catalysts. Catalysts 2018, 8, 149.

21. Luo, J.; Wang, D.; Kumar, A.; Li, J.; Kamasamudram, K.; Currier, N., Identification of two types of Cu sites in Cu / SSZ-13 and their unique responses to hydrothermal aging and sulfur poisoning. Catalysis Today 2016, 267, 3–9.

22. Colombo, M.;Nova, I.; Tronconi, E., Detailed kinetic modeling og the NH3-NO/NO2 SCR reactions over a commercial Cu-zeolite catalyst for Diesel exhausts after treatment. Catalysis Today 2012, 197, 243–255.

23. Ruggeri, M.P.; Selleri, T.; Colombo, M.; Nova, I.; Tronconi, E., Identification of nitrites/HONO as primary products of NO oxidation over Fe-ZSM-5 and their role in the Standard SCR mechanism: A chemical trapping study. Journal of Catalysis 2014, 311, 266–270.

24. Colombo, M.; Nova, I.; Tronconi, E., NO2 adsorption on Fe- and Cu-zeolite catalysts : The effect of the catalyst red – ox state. Applied Catalysis B: Environmental 2012, 111–112, 433–444 .

25. Mihai, O.; Widyastuti, C.R.; Andonova, S.; Kamasamudram, K.; Li, J.; Joshi, S.Y.; Yezerets, A.; Olsson, L., The effect of Cu-loading on different reactions involved in NH_3 -SCR over Cu-BEA catalysts. Journal of Catalysis 2014, 311, 170–181.

26. Hadjiivanov, K.; Klissurski, D.; Ramis, G.; Busca, G., Fourier transform IR study of NO_x adsorption on a CuZSM-5 $DeNO_x$ catalyst. Applied Catalysis B: Environmental 1996, 7, 251–267.

27. Negri, C.; Hammershoi, P.S.; Janssens, T.W.V.; Beato, P.; Berlier, G.; Bordiga, S., Investigating the low temperature formation of CuII-(N,O) species on Cu-CHA zeolites for the Selective Catalytic Reduction of NOx. Chemistry - A European Journal 2018, 24, 12044–12053.

28. Yuvaraj, S.; Fan-Yuan, L.; Tsong-Huei, C.; Chuin-Tih, Y., Thermal decomposition of Metal

nitrates in air and hydrogen environments. Journal of Physical Chemistry 2003, 107, 1044 (2003).

29. Bagnasco, G., Improving the Selectivity of NH_3 TPD Measurements. Journal of Catalysis 1996, 159, 249–252.

30. Gao, F.; Wang, Y.; Washton, N.M.; Peden, C.H.F., E ff ects of Alkali and Alkaline Earth Cocations on the Activity and Hydrothermal Stability of Cu / SSZ-13 NH_3 − SCR Catalysts. ACS Catalysis 2015, 5, 6780-6791.

31. Han, S.; Ye, Q.; Cheng, S.; Kang, T.; Dai, H., Effect of the hydrothermal aging temperature and Cu/Al ratio on the hydrothermal stability of Cu-SSZ-13 catalysts for the NH_3-SCR. Catalysis Science & Technology 2017, 7, 703–717.

32. Lezcano-Gonzalez, I.; Deka, U.; Arstad, B.; Van Yperen-De Deyne, A.; Hemelsoet, K.; Waroquier, M.; Van Speybroeck, V.; Weckhuysen, B.M.; Baele, A.M., Determining the storage, availability and reactivity of NH_3 within Cu-Chabazite-based Ammonia Seleective Catalytic Reduction systems. Physical Chemistry Chemical Physics 2014, 16, 1639 .